EBV-miR-BART12 accelerates cancer cell migration and invasion through targeting TPPP1 in EBV associated cancer

Yingfen Wu
Central South University
Fang Wei
Central South University
Dan Wang
Central South University
Le Tang
Central South University
Liting Yang
Central South University
Lei Shi
Central South University
Can Guo
Central South University
Fang Xiong
Central South University
Xiayu Li
Central South University
Xu Wu
Central South University
Zhaojian Gong
Central South University
Ming Zhou
Central South University
Bo Xiang
Central South University
Xiaoling Li
Central South University
Guiyuan Li
Central South University
Zhaoyang Zeng

Central South University

Wei Xiong (xiongwei@csu.edu.cn)

Central South University

Research

Keywords: EBV-miR-BART12, TPPP1, EMT, α-tubulin, β-catenin, EMT, NPC

Posted Date: December 12th, 2019

DOI: https://doi.org/10.21203/rs.2.18622/v1

Abstract

Background: Epstein-Barr virus (EBV) is suggested to actively utilize its EBV microRNAs (miRNAs) to manipulate viral and cellular functions during neoplasia transformation. But its role in tumor development and maintenance remains unclear. The objective of this study is to examine EBV-miRNA-BART12 implicated in EBV associated carcinogenesis.

Methods :Expression of EBV-miRNA-BART12 and TPPP1 (Tubulin Polymerization Promoting Protein 1) was confirmed by GEO datasets, RT-PCR and in situ hybridization. Luciferase analyses, RT-PCR and western blotting experiments examined and confirmed that EBV-miRNA-BART12 targeted the 3'-UTR of TPPP1 mRNA. Migration and invasion ability were measured by wound healing and transwell assay. And the mechanism was assessed by western blotting and immunofluorescence.

Results : Our results showed that EBV-miRNA-BART12 was highly expressed and TPPP1 was lowly expressed in NPC and/or GC and tightly associated with these patients' prognosis. Additionally, EBV-miR-BART12 advanced the HDAC6 (Histone Deacetylase 6) activity in cells by inhibiting TPPP1, and stimulated acetylation of α-tubulin and β-catenin, thereby increasing the microtubule instability and activating the epithelial-mesenchymal transition (EMT) process.

Conclusion : EBV-encoded BART12 promotes migration and invasion of EBV associated NPC and gastric cancer by inhibiting TPPP1 mRNA and promoting the microtubule instability and the cellular EMT process.

Background

The Epstein-Barr virus (EBV) is widespread within the human population with over 90% of adults being infected and closely associated with the development and progression of some lymphomas (1, 2), nasopharyngeal carcinoma (NPC)(3), and apart of gastric cancer (GC)(4, 5). It encodes 44 mature microRNAs (miRNAs), divided into two clusters: BHRFs and BARTs (6). BART miRNAs were shown to affect the malignant phenotype, including viral latency (7–10), immune escape(11), cell proliferation(12–16), cell apoptosis(15, 17), cell metastasis(18, 19). These findings suggest that EBV miRNAs may exert a variety of important regulatory functions in EBV-mediated tumorigenesis and cancer progression. Nevertheless, the functions of most EBV-encoded miRNAs remain to be elucidated.

We previously profiled all 44 EBV-encoded mature miRNAs in NPC biopsies and non-cancerous nasopharyngeal tissues and found that EBV miRNAs located in the BART region were highly expressed in NPC biopsies. EBV-miR-BART12 was highly expressed in NPC samples compared with non-tumor nasopharyngeal epitheliums (NPE). But its function in NPC is still unclear.

Tubulin polymerization promoting protein 1 (TPPP1) is a microtubule (MT) regulatory protein that drives MT polymerization and stabilization. It encodes 25-kDa protein and belongs to the tubulin polymerization promoting protein family that includes TPPP2 (p20) and TPPP3 (p18) (20, 21). Overexpression of TPPP1

in cells promotes MT polymerization and an increase in MT acetylation, whereas introduction of TPPP1 RNAi reduces MT acetylation. It binds to tubulin heterodimers and facilitates their incorporation into the growing microtubule filaments. It also binds to histone deacetylase 6 (HDAC6), a major MT deacetylase, and inhibits its activity leading to increased MT acetylation, a polymer stabilizing modification (22).

In this study, we tried to explore the function of EBV-miR-BART12 through TPPP1 gene on the microtubule network and the EMT process in three different cell lines. Our results suggested that TPPP1 was a direct target of EBV-miR-BART12. EBV-miR-BART12 decreased acetylation of the microtubule network and affected the stability of the microtubule network through TPPP1, as well as decreased acetylation of β-catenin and facilitated the EMT process, therefore resulting in increased cell migration and invasion.

Materials And Methods

Clinical samples

All tissue samples were collected by the Hunan Cancer Hospital for pathology studies. These samples were pathologically tested before used for study. Samples measuring EBV-miR-BART12 expression levels included 27 tumor tissue samples and 13 normal nasopharyngeal epithelial samples. Samples for detecting the TPPP expression level included 34 nasopharyngeal carcinoma samples and 24 normal nasopharyngeal epithelial samples.

Cell lines, plasmids, and chemicals

Cell lines were maintained in RPMI-1640 medium (Life Technologies, Grand Island, NY, USA) supplemented with 10% fetal bovine serum (Gibco, Invitrogen, Shanghai, China), penicillin (100U/ml, #P3032, Sigma Chemicals, St Louis, MO, USA) and streptomycin (100 g/ml, #WB11000, Sigma Chemicals) in a humidified incubator with 5% CO_2 at 37°C, including EBV negative cell lines 5-8F and AGS, and EBV positive cell line C666-1. The broad-spectrum HDAC inhibitor Trichostatin A (TSA) was purchased from Sigma (Sigma, St. Louis, MO). When indicated, the cells were treated with TSA (240 nM, overnight). HDAC6 specific inhibitor Tubacin (Tub, Selleck, Selleck Chemicals) was also used to treat cells (16 μM) for 24 h(23). For cold depolymerization, the cells were incubated at 4℃ for 30 min(23). For paclitaxel test, the cells were treated with 15 nM paclitaxel (PTX,) overnight. And PTX was purchased from Beijing Sihuan Kexing Biochemical Technology Co., Ltd. (Beijing, China).

Synthetic EBV-miR-BART12 mimics or inhibitors were products of Ruibo Company (RiboBioCo., Guangdong, China). EBV-miR-BART12 inhibitors were chemically synthesized, single-stranded, modified RNA molecules that can specifically inhibit endogenous target EBV-miR-BART12 miRNA. Both were worked at the concentration of 50 nM. Full-length cDNA of *TPPP1* gene was amplified by PCR and constructed by inserting a PCR product into IRESneo3 vector. *TPPP1* siRNAs were obtained from Genepharma (Genepharma, Shanghai, China) and worked at 100 nM concentration. The luciferase reporter was established by inserting synthetic oligonucleotides containing either the wild-type EBV-miR-

BART12 binding site in TPPP1 3'-UTR (TPPP1-WT) or the one with mutant-binding sites (TPPP1-MT) into the pMIR-Report luciferase vector (Ambion, Austin, TX,). The sequences of the synthetic oligonucleotides are listed in the Additional file 1. Transfection of plasmids and miRNAs was performed with Lipofectamine 3000 (Invitrogen, the Nederlands) or Hipefect (Qiagen, Hilden, Germany) as recommended.

GEO data

Multiple gene chips (GSE12452, GSE36682, GSE32960, GSE13195, GSE38749, and GSE26253) were downloaded from NCBI's GEO datasets for data analysis(24-27). We performed differential analysis of the data by the SAM software to select differentially expressed genes(28), and analyze the mRNA expression, the correlation between the expression level and the survival time by the GraphPad Prism software.

Wound healing and transwell assay

Wound healing: When the cells were grown to 90% confluence after transfection, a 10 μl pipet tip was used to create a scratch in the cell monolayer. Images of the scratched area were taken at the time point of 0 h, 12 h, 24 h, 36 h, and 48 h under a micro scope after wounding. Transwell assay: cells were seeded in the chamber (8 μm pores; Corning, NY) coated with Matrigel (BD Biosciences). Then the chamber was put into 24 well plates when the top chamber was added into serum-free medium whereas the bottom well was added into medium with 20% FBS. The plate was incubated at 37°C for 24 – 48 h and then the chambers were fixed with 4% paraformaldehyde for 10 min, invasive cells were examined by crystal violet staining, and observed under a microscope.

Quantitative real-time PCR (qRT-PCR)

Total RNA was isolated with TRIzol reagent (Invitrogen, Carlsbad, CA), according to manufacturer's protocol. For real-time PCR, cDNA was synthesized using miDETECTA Track™ miRNA qRT-PCR system (RiboBio, Guangzhou, China), following manufacturer's instructions. The expression level of EBV-miR-BART12 was measured by RiboBio miRNA primer assays (RiboBio, Guangzhou, China) using the miDETECTA Track™ miRNA qRT-PCR system (RiboBio, Guangzhou, China), in compliance with manufacturer's instructions. Data was normalized to the expression level of small nuclear RNA RNU6B (U6 snRNA). Real-time PCR for *TPPP1* was carried out using a SYBR green real-time PCR kit (Applied Biological Materials, BC, Canada). Data were normalized to the expression level of GAPDH and further normalized to the negative control, unless indicated. The primers used for PCR listed in Additional file 1. The fold changes were calculated by the relative quantification($2^{-\Delta\Delta}$Ct) method. All reactions were run in triplicate and repeated in three independent experiments.

Western blotting

The protein was extracted using the Radio-Immunoprecipitation Assay Buffer (RIPA buffer, SantaCruz, CA) and the protein concentration was determined using the BCA Protein Assay Kit (Pierced, Grand Island, NY). Samples were separated by electrophoresis on 10-12% sodium dodecylsulfate (SDS) polyacrylamide gels, and the separated proteins were transferred to a polyvinylidenefluoride (PVDF) membrane (Millipore, Billerica, MA). To assess the protein expression, the blots were incubated with the following primary antibodies at 4℃ overnight: rabbit antibodies against TPPP1 (Proteintech,Wuhan, China), β-catenin (Cell Signaling Technology, Danvers, MA), the EMT kit antibodies（Cell Signaling Technology, Danvers, MA）and acetylated β-catenin (Cell Signaling Technology, Danvers, MA), as well as mouse antibodies against GAPDH (Cell Signaling Technology, Danvers, MA), α-tubulin (Proteintech, Wuhan, China), and acetylated α-tubulin (Proteintech, Wuhan, China). After washing, the blots were incubated with horseradish peroxidase-conjugated anti-rabbit secondary antibodies (Santa Cruz, Heidelberg, Germany) at a dilution of 1:2000 for 1 h at room temperature. Blots were visualized by exposure to X-ray film, through an enhanced chemiluminescence detection system (Millipore, Darmstadt, Germany), and quantified by densitometry using the Image J software (http://rsb.info.nih.gov/ij). GAPDH served as an endogenous control for equal loading and Histone H3 served as a nucleus control.

Bioinformatics analysis and luciferase assay

The putative targets of miRNAs were analyzed using the following respective databases: Reptar (http://reptar.ekmd.huji.ac.il/), PITA (http://genie.weizmann.ac.il/pubs/mir07/mir07_data.html), RNAhybrid (http://bibiserv.techfak.uni-bielefeld.de/rnahybrid/), and RNA22 (https://cm.jefferson.edu/rna22/Interactive/).

Cells were plated into each well of a 24-well plate and then co-transfected with synthetic EBV-miR-BART12 mimics and luciferase reporter plasmids (either TPPP1-WT or TPPP1-Mutant), also along with pRL-TK renilla luciferase vector (Promega, Madison, WI). Luciferase activity was measured using the Dual-Luciferase® Reporter Assay System (Promega, Madison, WI). All experiments were performed three times.

In situ hybridization (ISH) and immunohistochemistry (IHC)

ISH and IHC staining were performed as previously described(29). Paraffin sections were first dewaxed, then paraffin was removed from the turpentine, and the turpentine was washed with gradient alcohol and the slices was hydrated. For ISH, tissue sections were first inactivated by H_2O_2 to inactivate endogenous peroxidase, fixed by 4% paraformaldehyde, digested by pepsin diluted with 3% citric acid, and then pre-hybridized and hybridized, followed by blocking, and biotinylated rat anti- digoxin, SABC(strept avidin-biotin complex) and biotinylated peroxidase were added dropwise to tissues, final DAB (Diaminobenzidine) color development, hematoxylin counterstaining, gradient alcohol dehydration,

neutral resin sealing. For IHC, the tissue sections were firstly subjected to antigen retrieval, and then 3% H_2O_2 was used to inactivate endogenous peroxidase. After blocking for 30 min, the TPPP1 primary antibody was incubated overnight. After rewarming at room temperature, the secondary antibody was incubated for 30 min, DAB was colored, and hematoxylin was counterstained. Finally, neutral resin seals the tissues. Sequences of EBV-miR-BART12 probe could be seen in Additional file 1.

Animal experiments

Four-week-old male BALB/c nude mice with weight 20±2g were purchased from and raised at the Laboratory Animal Services Centre of Central South University with specific pathogen free. Animal handling and experimental procedures were approved by the Animal Experimental Ethics Committee of Central South University. Forty mice were randomly divided into four groups. To determine the lung metastatic potential of cancer cells in vivo, cells (1 10^6 cells /200 μL) transfected with Saline, EBV-miR-BART12 mimics, TPPP1-overexpression vector or TPPP1 siRNA were injected through the tail vein when they were five weeks old. The mice were all sacrificed 2 months later by cervical dislocation, and the lung were removed for following experiments.

Immunofluorescence

Cells were seeded at glass coverslips in 6-well plates and incubated for 24 h. After incubation, cells were treated with TSA for 24 h and then fixed with 4% paraformaldehyde and permeabilized with 0.5% Triton X-100 for 10 min to remove the soluble proteins and washed three times with PBS. The coverslips were incubated with primary antibodies overnight. Immunofluorescence was done using α-tubulin (1:200), acetylated tubulin (Lys40) (1:200), TPPP1 (1:200) antibody. The cells were incubated with secondary antibodies for 1 h at 37 ℃ and 49,6-diamidino-2-phenylindole (DAPI) for 10 min at room temperature. The coverslips were mounted on glass slides. Immunofluorescence images were collected using a confocal fluorescence microscope (UltraView Vox; PerkinElmer, Waltham, MA, USA).

Statistics analyses

Statistical analysis was performed using software of GraphPad Prism 5 (GraphPad, LaJolla, CA). Student's t-tests were used to evaluate significant differences between any two groups of data. One-way ANOVA was used when there are more than two groups. Survival estimates overtime were calculated using the Kaplan-Meier method, and the differences were compared using the log-rank test. The results of the analysis were considered significant in a log-rank test if $P < 0.05$.

Results

The expression of EBV-miR-BART12 and TPPP1 was associated with the poor prognosis of NPC or GC patients.

First, the NPC online GEO data (GSE36682 and GSE32960) were used to analyze the expression level of EBV-miR-BART12, which was highly expressed in the NPC tissues (Figure 1A), compared with the adjacent nasopharyngeal normal tissues. Then the expression of EBV-miR-BART12 was confirmed in 40 clinical samples including 27 NPCs and 13 normal nasopharyngeal epitheliums by qRT-PCR. EBV-miR-BART12 was highly expressed in these NPC clinical samples (Figure 1B). The expression of EBV-miR-BART12 was also associated with the poor prognosis in these NPC patients, in which high EBV-miR-BART12 expression patients had a lower survival rate in GSE36682 (Figure 1C).

The bioinformatics software was used and predicted that TPPP1 gene was the potential target of EBV-miR-BART12 (Additional file 2). The GEO data GSE12452 (NPC) and GSE13195 (GC) showed that the expression of TPPP1 in cancers was lower than the non-tumor tissues (Figure 1D). The qRT-PCR data also showed TPPP1 was lowly expressed in 34 NPC tissues compared with 24 NPE tissues (Figure 1E). The expression of TPPP1 was tightly associated with the survival time of GC patients in GSE26253, the low TPPP1 expression patients with the short survival rate (Figure 1F). The ISH and IHC results also show that EBV-miR-BART12 was highly expressed in NPC, while TPPP1 is just found in NPE part (Figure 1G). Then we predicted through the bioinformatics software that TPPP1 was one of the targets of EBV-miR-BART12 and found that TPPP1 was also down-regulated in NPC of GSE12452 (Figure 1H, Additional file 3).

We concluded that the expression of EBV-miR-BART12 and TPPP1 might be correlated with the survival rate of NPC or GC patients. Metastasis is one of the reasons for the death of cancer patients. Therefore, we speculate that EBV-miR-BART12 may affect the migration and invasion of EBV associated tumors by targeting the TPPP1, which plays an important role in the development of malignant tumors.

EBV-miR-BART12 inhibits TPPP1 expression through directly targeting TPPP1 3’-UTR

According to the above results, we tried to confirm if EBV-miR-BART12 targets the 3’-UTR of TPPP1 mRNA. Firstly, the EBV-miR-BART12 chemical synthesis analogues (EBV-miR-BART12 mimics) were transfected into EBV negative NPC 5-8F and GC AGS cell lines. EBV-miR-BART12 was overexpressed in the experimental group, while it was not detected in the control group (Figure 2A). Meanwhile, EBV-miR-BART12 inhibitors were also transfected into EBV positive NPC C666-1 cell lines and the qRT-PCR results showed that the inhibitors reduce the expression of EBV-miR-BART12. Then the expression of TPPP1 in 5-8F, AGS, C666-1 was also detected by qRT-PCR after transfection of EBV-miR-BART12 mimics or inhibitors. The TPPP1 mRNA was reduced after EBV-miR-BART12 mimics or induced after the inhibitor’s transfection (Figure 2B). Western Blotting also confirmed that the expression of TPPP1 was inhibited by EBV-miR-BART12 mimics in 5-8F and AGS cell lines and promoted by EBV-miR-BART12 inhibitors in

C666-1 cell lines (Figure 2C). In order to detect whether EBV-miR-BART12 directs to target TPPP1, the bioinformatics software was used, including: RepTar, RNAhybrid, RNA22, and PITA. There were four binding sites of the TPPP1 3'-UTR predicted, including 1401-1423 bp, 2809-2898 bp, 3642-3908 bp, and 4533-4565 bp. The sequence 1401-1423 bp was selected to construct the luciferase reporter vector of wild type (TPPP1-WT) through inserting into the pMIR-Report luciferase vector, or the sequence of partial missing sequences was constructed as a TPPP1 mutant vector (TPPP1-MT, Figure 2D). The luciferase values in 5-8F and AGS cell lines co-transfected with EBV-miR-BART12 mimics and the TPPP1-WT were significantly lower than those in the control group, while the values of luciferase in co-transfected EBV-miR-BART12 mimics and the TPPP1-MT cells were unchanged. This showed that EBV-miR-BART12 mimics play its inhibitory effect by directly targeting the 3'-UTR of TPPP1 (Figure 2E). EBV-miR-BART12 inhibitors increased the luciferase activities of TPPP1-WT but no effect in TPPP1-MT (Figure 2E). These experimental results indicated that EBV-miR-BART12 directly combined with the 3'-UTR of TPPP1.

EBV-miR-BART12 promotes migration and invasion of cancer cells by inhibiting TPPP1

Metastasis is an important feature of tumor cells. We speculate that EBV-miR-BART12 affects migration and invasion of tumor cells through downregulating the expression of TPPP1. To verify this hypothesis, the scratch test and transwell assay were executed in 5-8F and AGS cell lines through transfecting with EBV-miR-BART12 mimics (BART12), the TPPP1 overexpression vector (TPPP1), TPPP1 siRNA (siTPPP1), or co-transfecting EBV-miR-BART12 mimics and the TPPP1 over expression vector (BART12 + TPPP1) to measure the ability of migration and invasion. The effect of transfection of these materials on intracellular TPPP1 mRNA is shown in the Supplementary Figure 2. The results showed that EBV-miR-BART12 and siTPPP1 increased the migration and invasion ability in 5-8F, while the TPPP1 decreased it. Similar results were also seen in AGS (Figure 3A and B). The TPPP1 overexpression vector reversed the ability of EBV-miR-BART12 mimics after co-transfection of EBV-miR-BART12 mimics and the TPPP1 overexpression vector. These results suggested that EBV-miR-BART12 promoted tumor cells migration and invasion through down-regulating TPPP1. In C666-1, EBV-miR-BART12 inhibitors (BART12 In), the TPPP1 overexpression vector (TPPP1), TPPP1 siRNA (siTPPP1), or EBV- miR-BART12 inhibitors combined with TPPP1 siRNA (BART12 In + siTPPP1) were also transfected. The results of scratch test and the transwell assay showed that EBV-miR-BART12 inhibitors reduced the ability of migration and invasion. Overexpression of TPPP1 also inhibited and siTPPP1 boosted the migration and invasion of C666-1(Figure 3A and 3B). We conclude that EBV-miR-BART12 promotes the migration and invasion of cancer cells by inhibiting TPPP1.

EBV-miR-BART12 impacts the microtubules dynamic instability by affecting TPPP1.

TPPP1 is a microtubule related protein which affects the dynamics and stability of the microtubule network through interacting with microtubules. On the one hand, TPPP1 promotes tubulin polymerization and microtubule bundles by its polymerization activity, on the other hand, TPPP1 influences microtubules acetylation level through binding with microtubule deacetylase. In order to explore whether EBV-miR-BART12 affects the microtubule dynamic stability through targeting TPPP1, the microtubule network morphology was detected in five groups, including control, BART12, TPPP1, siTPPP1, BART12 + TPPP1 group (Figure 4A). The results showed that TPPP1 mainly distributed in cytoplasm. The green fluorescence representing the TPPP1 expression was significantly lower than the control group in the cells after EBV-miR-BART12 mimics transfection, indicating that TPPP1 expression was significantly decreased, and the content of tubulin represented by the red fluorescence was also reduced. Tubulin gathered around the nucleus and cytoplasm was scattered after EBV-miR-BART12 mimics transfection and was no longer the rules of radial distribution which was in the control group. After over expression of TPPP1, the green fluorescence value of TPPP1 was also significantly increased. The content of TPPP1 on the edge of cells increased, and the expression of microtubule protein increased correspondingly. The morphological changes of the cells suggested that EBV-miR-BART12 might be associated with apoptosis and metastasis. The cells had shrunken to a smaller circle. The morphological changes and infection of the group siTPPP1 were like that of the group BART12 (Figure 4A).

In addition, western blotting also showed that the acetylated α-tubulin was inhibited by EBV-miR-BART12 mimics and siTPPP1 and induced by TPPP1 (Figure 4B), which hinted that EBV-miR-BART12 reduced the acetylation through targeting TPPP1. Immunofluorescence showed that acetylated α-tubulin and TPPP1 were colocalized with each other in the control group. After transfection of EBV-miR-BART12 mimics, the expression of TPPP1 significantly decreased compared to that of the control group. And the expression and distribution of acetylated α-tubulin was significantly different from the control group. In the EBV-miR-BART12 group, the distribution of acetylated α-tubulin decreased, while the density increased, and the cell shrinkage became smaller and round. After overexpression of TPPP1, the expression of TPPP1 in cells was significantly higher than that in control cells, with higher density and full in the cytoplasm, while the morphology of acetylated α-tubulin was more complete. The results for the EBV-miR-BART12 + siTPPP1 group were like those in the TPPP1 group, while the results of the siTPPP1 group were like those in the EBV-miR-BART12 group (Figure 4C). From these results, we concluded that EBV-miR-BART12 affected the distribution, expression and acetylation degree of α-tubulin by downregulating the expression of TPPP1. This affects the microtubule network dynamic stability.

EBV-miR-BART12 influences the stability of microtubules by down-regulating of TPPP1.

Acetylation of microtubules is an important indicator for evaluating microtubule stability. The stable microtubules usually have a higher degree of acetylation. In order to observe the distribution and expression of acetylated α-tubulin in cells more clearly, immunofluorescence was used to observe the expression and distribution of α-tubulin and acetylated α-tubulin in cells to explore the effect of EBV-miR-

BART12 on the stability and dynamics of microtubule. In these experiments, the HDAC6 inhibitor TSA was used to treat cells. In the control group, α-tubulin and the acetylated α-tubulin were partly co-localized in the perinuclear region. When the 5-8F cells were treated with EBV-miR-BART12 mimics, the luminance of acetylated α-tubulin was lower than that of the control group. After the entry of TSA, the brightness of acetylated α-tubulin increased, and cold treated TSA cells resistant this increasing (Figure 5A).

Similarly, western blotting experiments were performed to observe the changes of acetylated α-tubulin after treated with or without TSA on 5-8F and AGS cell lines transfected with EBV-miR-BART12 mimics (BART12) or C666-1 with EBV-miR-BART12 inhibitors (BART12 In), the TPPP1 overexpression vector (TPPP1) and TPPP1 siRNA(siTPPP1). It was found that TSA increased the acetylation of α-tubulin to a higher level in negative control cells, and the expression of acetylated α-tubulin protein in the control group was higher than that of TSA-treated BART12 group and lower than that of the TSA-treated BART12 In group. The expression of acetylated α-tubulin protein in the siTPPP1 group was consistent with the BART12 group. In the TPPP1 group, the addition of TSA further encouraged acetylation of α-tubulin (Figure 5B). In summary, TSA, an inhibitor of HDAC6, is resistant to microtubule depolymerization by cold treatment, which is produced by acetylated α-tubulin. EBV-miR-BART12 reduced the content of acetylated α-tubulin. Therefore, EBV-miR-BART12 promoted the increase of HDAC6 content in cells through down-regulating the expression of TPPP1, leading to the down-regulation of microtubule acetylation in cells and the decrease of microtubule network stability and anti-depolymerization ability, which causes the migration and invasion of tumor cells. Then HDAC6 specific inhibitor Tubacin (Tub) was also used to treat cells and the results was consistent with TSA (Figure 5C).

Paclitaxel (PTX) is a famous antitumor chemotherapeutic drug, which promotes the assembly of free tubulin subunits into microtubules and facilitates microtubule stabilization by binding to microtubules(30). To test whether paclitaxel influences EBV-miR-BART12-associated NPC and GC or not, we examined the expression of α-tubulin and acetylated α-tubulin in cells treated with paclitaxel by western blotting. The results showed that paclitaxel did cause an increase in the protein expression levels of α-tubulin and acetylated α-tubulin. However, EBV-miR-BART12 group cells, with paclitaxel treatment, had little effect on the expression level of α-tubulin, but it greatly increased the expression level of acetylated α-tubulin (Figure 5C). The results indicate that paclitaxel does not have a particularly good effect on the reduction of microtubules caused by EBV-miR-BART12 but can greatly enhance the stability of the remaining microtubule network. It is suggested that clinical treatment with paclitaxel will have a certain effect on the progression of NPC and GC. In summary, EBV-miR-BART12 promotes deacetylation of microtubules and increases microtubule instability by binding and down-regulating the expression of TPPP1.

EBV-miR-BART12 induces the EMT process by restraining the inhibitory effect of TPPP1 on β-catenin

TPPP1 promotes the degradation of β-catenin by inhibiting the activity of HDAC6(31).So we examined if the expression of acetylated β-catenin was regulated by EBV-miR-BART12 through TPPP1 gene in 5-8F, AGS, and C666-1 cell lines. The results showed that EBV-miR-BART12 reduced acetylation of β-catenin through TPPP1 gene (Figure 6A). So, 5-8F, AGS, and C666-1 cell lines were treated with the HDAC6 inhibitor TSA or Tub after EBV-miR-BART12 mimics or inhibitors transfected into cells to detect whether EBV-miR-BART12 regulate the expression of acetylated β-catenin through interacting with TPPP1 and HDAC6. The western blotting results showed that TSA increased the expression of total β-catenin and reduced the protein level of acetylated β-catenin. EBV-miR-BART12 decreased the expression of acetylated β-catenin. After adding TSA or Tub to medium, the expression of acetylated β-catenin increased in the EBV-miR-BART12 mimics group, but it was still lower than that of the control group (Figure 6B - 6E). The results showed that the activity of HDAC6 in the cells was inhibited by TSA, and the effect of EBV-miR-BART12 on β-catenin and acetylated β-catenin was inhibited. On the other hand, it was indicated that EBV-miR-BART12 decreased the expression of TPPP1 and inhibited the function of TPPP1 and HDAC6, thereby promoting the deacetylation of β-catenin and making the β-catenin free from the fate of proteasome degradation.

Also, β-catenin is a key marker of the EMT signaling pathway. We speculate that EBV-miR-BART12 participates in the EMT signaling pathway by protecting β-catenin from degradation, promoting the activation of β-catenin and its downstream molecules. To this end, we detected the expression of some EMT related molecules in 5-8F and AGS cell lines with BART12, the TPPP1, or siTPPP1 groups. The results showed that E-cadherin, Claudin-1, and ZO-1 were down-regulated, transcription factors 4 (TCF4), N-cadherin, Vimentin, Slug, and Snail were upregulated in the EBV-miR-BART12 group. They are opposite to the TPPP1 group (Figure 6E). The qRT-PCR results also showed the same trend of these EMT molecules (Figure 6F). These results suggest that EBV-miR-BART12 stimulates the EMT process through downregulating the expression of TPPP1, and reducing the binding of TPPP1 and HDAC6, then resulting in the activation of β-catenin.

Finally, we detected the distribution of β-catenin expression in 5-8F, AGS, and C666-1 cells in order to prove if EBV-miR-BART12 promotes the EMT process through regulating β-catenin entering the nucleus. The histone H3 is a nuclear reference and α-tubulin works as a cytoplasmic reference. The results showed that EBV-miR-BART12 increased the expression of β-catenin in the nucleus and cytoplasm, compared with the control group (Figure 6G). The results above indicate that EBV-miR-BART12 enhances the activity of HDAC6 by inhibiting the expression of TPPP1, thereby promoting the deacetylation of β-catenin, accelerating the enucleation of β-catenin, and finally initiating the downstream transcription factor to facilitate the EMT process.

Discussion

In this study, we found that EBV-miR-BART12 was highly expressed in the NPC clinical samples and positively correlated with the prognosis of the NPC patients. It deacetylated α-tubulin and β-catenin,

resulting in microtubules polymerization and β-catenin entering the nucleus and activation. Thereby promoting the EMT process through directly targeting the 3'-UTR of TPPP1 mRNA.

TPPP1 is a microtubule associated protein (MAPs), which promote tubulin proteins aggregating into microtubules and changing the ultra-structure of microtubule (32). The present studies showed that TPPP1 affected cell cycle and migration through regulating the microtubule, although there is still very few reports in cancer research(33–38). It is reported that TPPP1 was low-expressed in oligodendrocyte gliomas(39), non-small cell lung cancer(40), and hepatocellular carcinoma(41) and associated with poor prognosis of the patients(31, 41, 42), suggesting that TPPP1 be used as a potential molecular cancer marker and potential target. In this study, we preliminarily study the mechanism of TPPP1 in tumorigenesis. EBV-miR-BART12 regulates the microtubule dynamic stability and EMT process in cancer cells through targeting TPPP1.

As one of the cytoskeleton component, the microtubule stability affects cancer cells invasion and metastasis (37, 43). The co-localization of TPPP1 and α-tubulin proteins increases the microtubule stability(29). Many factors affect the microtubules stability including the posttranslational modification and some microtubule proteins. Microtubules in a stable state will gather more posttranslational modifications, such as microtubule acetylation (44, 45). The regulation of acetylation is an important function of TPPP1. TPPP1 stabilized microtubules and promoted tubulin acetylation through binding and inhibiting HDAC6 activity(37, 46). The interaction between HDAC6 and TPPP1 led to the inhibition of HDAC6 deacetylation activity, and thus increased the microtubule acetylation. In this study, we found that TPPP1 and α-tubulin were co-localized in the cytoplasm. EBV-miR-BART12 affects acetylation of microtubules by binding TPPP1, causing the change of the microtubule structure.

It had been reported that HDAC6 also be involved in the formation of tumors by deacetylating other molecules, such as β-catenin(47) and then promoting the nuclear localization of β-catenin(47, 48), the EMT process(49) and tumor invasion and metastasis(50). As an inhibitor of HDAC6, TPPP1 was decreased by EBV-miR-BART12, causing an increase of HDAC6 activity. When HDAC6 activity is elevated, the acetylation level of β-catenin is decreased, which reduces the amount of β-catenin that should be degraded. Then the level of β-catenin in the cytoplasm is improved, which promotes the entry of β-catenin into the nucleus, activates downstream transcription factors, and initiates EMT, thereby facilitating tumor cell invasion and metastasis.

In this study, we combined with clinical chemotherapeutic drugs to analyze the prospects of EBV-miR-BART12 in tumor therapy. Paclitaxel is a chemotherapeutic agent (30, 32, 51), which has strong anti-tumor ability in clinic mainly through promoting the assembly of microtubules and stabilizing the polymerized microtubules, resulting in stagnating cells in G0/G1 and G2/M stages and inducing apoptosis(52, 53). It has been widely used to treat solid tumors, including breast cancer, ovarian cancer, and non-small cell lung cancer, because of its curative effect and small side effects(54–56). In this study, EBV-miR-BART12 had an antagonistic effect on the microtubule with paclitaxel in cancer cells. EBV-miR-BART12 might promote microtubule depolymerization by inhibiting the expression of TPPP1, but this

depolymerization is reversed with the action of paclitaxel. It is suggested that paclitaxel may be effective in the treatment of patients with high expression of EBV-miR-BART12. And the development of a combination of EBV-miR-BART12 inhibitors and paclitaxel has a potential effect on the treatment of EBV related NPC and gastric cancer.

Conclusion

We have found the high expression of EBV-miR-BART12 is related to the poor prognosis of the NPC patients for the first time. EBV-miR-BART12 promoted NPC and GC cells through targeting the 3'-UTR of TPPP1 mRNA, resulting in an increasing the activity of HDAC6, and a deacetylation of α-tubulin and β-catenin, thereby changing the microtubules dynamic stability and promoting the EMT process, ultimately cancer migration and invasion (Supplementary Fig. 1). We also confirmed our results in the mouse experiment, too (Supplementary Fig. 2B). EBV-miR-BART12 and TPPP1 might be potential markers for the diagnosis and prognosis of NPC and GC and provided potential targets in NPC and GC treatment.

Abbreviations

EBV: Epstein-Barr virus **miRNAs:** microRNAs **NPC:** nasopharyngeal carcinoma **GC:** gastric cancer **TPPP1:** Tubulin Polymerization Promoting Protein **HDAC6:** Histone Deacetylase 6 **MT:** microtubule **EMT:** epithelial-mesenchymal transition **ISH:** *in situ* hybridization **IHC:** immunohistochemistry **SABC:** strept avidin-biotin complex **DAB:** diaminobenzidine **HE:** hematoxylin-eosin **Tub:** Tubacin **PTX:** Paclitaxel **TSA:** Trichostatin A **TCF4:** transcription factors 4

Declarations

Ethics approval and consent to participate

Not applicable.

Consent for publication

All authors read and approved the final manuscript.

Availability of data and materials

All data generated or analyzed during this study are included in this published article, and its supplementary information files.

Competing interests

The authors declare that they have no competing interests.

Funding

This work was supported in part by grants from the National Natural Science Foundation of China (81572787, 81672683, 81672993, 81772928, 81702907, 81772901, 31741049, 21806186 and 81872278), the Overseas Expertise Introduction Project for Discipline Innovation (111 Project, No. 111-2-12), and the Natural Science Foundation of Hunan Province (2016JC2035, 2017SK2105, 2018JJ3815, 2018JJ3704, 2018SK21210, and 2018SK21211).

Authors' contributions

YFW and ZYZ designed this study and drafted the manuscript. YFW performed the main experiments, FW, LT and DW helped with the western blotting parts. FW and LTY provided experimental guidance. ZYZ and WX revised this manuscript. LS, FX, XYL, ZJG, MZ, BX, XLL, XW, CG, GYL provided experimental assistance and suggestions. All authors read and approved the final manuscript.

Acknowledgements

Not applicable.

References

1. Roschewski M, Wilson WH. EBV-associated lymphomas in adults. Best practice & research Clinical haematology. 2012;25(1):75-89.
2. Dolcetti R, Dal Col J, Martorelli D, Carbone A, Klein E. Interplay among viral antigens, cellular pathways and tumor microenvironment in the pathogenesis of EBV-driven lymphomas. Seminars in Cancer Biology. 2013;23(6, Part A):441-56.
3. Senba M, Zhong XY, Senba MI, Itakura H. EBV and nasopharyngeal carcinoma. Lancet. 1994;343(8905):1104.
4. Oh ST, Seo JS, Moon UY, Kang KH, Shin DJ, Yoon SK, et al. A naturally derived gastric cancer cell line shows latency I Epstein-Barr virus infection closely resembling EBV-associated gastric cancer. Virology. 2004;320(2):330-6.
5. Iizasa H, Nanbo A, Nishikawa J, Jinushi M, Yoshiyama H. Epstein-Barr Virus (EBV)-associated gastric carcinoma. Viruses. 2012;4(12):3420-39.
6. Barth S, Meister G, Grasser FA. EBV-encoded miRNAs. Biochimica et biophysica acta. 2011;1809(11-12):631-40.
7. Barth S, Pfuhl T, Mamiani A, Ehses C, Roemer K, Kremmer E, et al. Epstein-Barr virus-encoded microRNA miR-BART2 down-regulates the viral DNA polymerase BALF5. Nucleic acids research. 2008;36(2):666-75.
8. Qiu J, Thorley-Lawson DA. EBV microRNA BART 18-5p targets MAP3K2 to facilitate persistence in vivo by inhibiting viral replication in B cells. Proceedings of the National Academy of Sciences of the United States of America. 2014;111(30):11157-62.

9. Jung YJ, Choi H, Kim H, Lee SK. MicroRNA miR-BART20-5p Stabilizes Epstein-Barr Virus Latency by Directly Targeting BZLF1 and BRLF1. Journal of Virology. 2014;88(16):9027-37.
10. Qiu J, Thorley-Lawson DA. EBV microRNA BART 18-5p targets MAP3K2 to facilitate persistence in vivo by inhibiting viral replication in B cells. Proceedings of the National Academy of Sciences. 2014;111(30):11157-62.
11. Lung RW-M, Tong JH-M, Sung Y-M, Leung P-S, Ng DC-H, Chau S-L, et al. Modulation of LMP2A Expression by a Newly Identified Epstein-Barr Virus-Encoded MicroRNA miR-BART22. Neoplasia. 2009;11(11):1174-IN17.
12. Ramakrishnan R, Donahue H, Garcia D, Tan J, Shimizu N, Rice AP, et al. Epstein-Barr Virus BART9 miRNA Modulates LMP1 Levels and Affects Growth Rate of Nasal NK T Cell Lymphomas. PLoS ONE. 2011;6(11):12.
13. Lei T, Yuen K-S, Xu R, Tsao SW, Chen H, Li M, et al. Targeting of DICE1 tumor suppressor by Epstein-Barr virus-encoded miR-BART3* microRNA in nasopharyngeal carcinoma. International Journal of Cancer. 2013;133(1):79-87.
14. Ambrosio M, Navari M, Di Lisio L, Leon E, Onnis A, Gazaneo S, et al. The Epstein Barr-encoded BART-6-3p microRNA affects regulation of cell growth and immuno response in Burkitt lymphoma. Infectious Agents and Cancer. 2014;9(1):12.
15. Kim H, Choi H, Lee SK. Epstein–Barr virus miR-BART20-5p regulates cell proliferation and apoptosis by targeting BAD. Cancer Letters. 2015;356(2):733-42.
16. Chen R, Zhang M, Li Q, Xiong H, Liu S, Fang W, et al. The Epstein-Barr Virus-encoded miR-BART22 targets MAP3K5 to promote host cell proliferative and invasive abilities in nasopharyngeal carcinoma. Journal of Cancer. 2017;8(2):305-13.
17. Choi H, Lee H, Kim SR, Gho YS, Lee SK. Epstein-Barr Virus-Encoded MicroRNA BART15-3p Promotes Cell Apoptosis Partially by Targeting BRUCE. Journal of Virology. 2013;87(14):8135-44.
18. Cai LM, Lyu XM, Luo WR, Cui XF, Ye YF, Yuan CC, et al. EBV-miR-BART7-3p promotes the EMT and metastasis of nasopharyngeal carcinoma cells by suppressing the tumor suppressor PTEN. Oncogene. 2015;34(17):2156-66.
19. Yan Q, Zeng Z, Gong Z, Zhang W, Li X, He B, et al. EBV-miR-BART10-3p facilitates epithelial-mesenchymal transition and promotes metastasis of nasopharyngeal carcinoma by targeting BTRC. Oncotarget. 2015;6(39):41766-82.
20. Orosz F. A new protein superfamily: TPPP-like proteins. PloS one. 2012;7(11):e49276.
21. Vincze O, Tokesi N, Olah J, Hlavanda E, Zotter A, Horvath I, et al. Tubulin polymerization promoting proteins (TPPPs): members of a new family with distinct structures and functions. Biochemistry. 2006;45(46):13818-26.
22. Tokesi N, Lehotzky A, Horvath I, Szabo B, Olah J, Lau P, et al. TPPP/p25 promotes tubulin acetylation by inhibiting histone deacetylase 6. The Journal of biological chemistry. 2010;285(23):17896-906.
23. Asthana J, Kapoor S, Mohan R, Panda D. Inhibition of HDAC6 Deacetylase Activity Increases Its Binding with Microtubules and Suppresses Microtubule Dynamic Instability in MCF-7 Cells. Journal

of Biological Chemistry. 2013;288(31):22516-26.

24. Sengupta S, den Boon JA, Chen IH, Newton MA, Dahl DB, Chen M, et al. Genome-Wide Expression Profiling Reveals EBV-Associated Inhibition of MHC Class I Expression in Nasopharyngeal Carcinoma. Cancer Research. 2006;66(16):7999.
25. Zhang N, Wang X, Huo Q, Li X, Wang H, Schneider P, et al. The Oncogene Metadherin Modulates the Apoptotic Pathway Based on the Tumor Necrosis Factor Superfamily Member TRAIL (Tumor Necrosis Factor-related Apoptosis-inducing Ligand) in Breast Cancer. Journal of Biological Chemistry. 2013;288(13):9396-407.
26. Pasini FS, Zilberstein B, Snitcovsky I, Roela RA, Mangone FRR, Ribeiro U, Jr., et al. A gene expression profile related to immune dampening in the tumor microenvironment is associated with poor prognosis in gastric adenocarcinoma. Journal of gastroenterology. 2014;49(11):1453-66.
27. Lee J, Sohn I, Do I-G, Kim K-M, Park SH, Park JO, et al. Nanostring-based multigene assay to predict recurrence for gastric cancer patients after surgery. PloS one. 2014;9(3):e90133.
28. Tusher VG, Tibshirani R, Chu G. Significance analysis of microarrays applied to the ionizing radiation response. Proceedings of the National Academy of Sciences of the United States of America. 2001;98(9):5116-21.
29. Lehotzky A, Tirián L, Tökési N, Lénárt P, Szabó B, Kovács J, et al. Dynamic targeting of microtubules by TPPP/p25 affects cell survival. Journal of Cell Science. 2004;117(25):6249.
30. Eric K. Rowinsky LAC, Ross C. Donehower. Taxol_ A novel investigational antimicrotubule. Journal of National Cancer Institute. 1990;82(15):1247-59.
31. Schofield AV, Gamell C, Bernard O. Tubulin polymerization promoting protein 1 (TPPP1) increases β-catenin expression through inhibition of HDAC6 activity in U2OS osteosarcoma cells. Biochemical and Biophysical Research Communications. 2013;436(4):571-7.
32. Kundranda M, Niu J. Albumin-bound paclitaxel in solid tumors: clinical development and future directions. Drug Design, Development and Therapy. 2015:3767.
33. Oláh J, Ovádi J. Dual life of TPPP/p25 evolved in physiological and pathological conditions. Biochemical Society Transactions. 2014;42(6):1762-7.
34. Schofield AV, Steel R, Bernard O. Rho-associated Coiled-coil Kinase (ROCK) Protein Controls Microtubule Dynamics in a Novel Signaling Pathway That Regulates Cell Migration. Journal of Biological Chemistry. 2012;287(52):43620-9.
35. Heng YW, Lim HH, Mina T, Utomo P, Zhong S, Lim CT, et al. TPPP acts downstream of RhoA-ROCK-LIMK2 to regulate astral microtubule organization and spindle orientation. Journal of Cell Science. 2012;125(6):1579-90.
36. Tirian L, Hlavanda E, Olah J, Horvath I, Orosz F, Szabo B, et al. TPPP/p25 promotes tubulin assemblies and blocks mitotic spindle formation. Proceedings of the National Academy of Sciences. 2003;100(24):13976-81.
37. Schofield AV, Gamell C, Suryadinata R, Sarcevic B, Bernard O. Tubulin Polymerization Promoting Protein 1 (Tppp1) Phosphorylation by Rho-associated Coiled-coil Kinase (Rock) and Cyclin-

dependent Kinase 1 (Cdk1) Inhibits Microtubule Dynamics to Increase Cell Proliferation. Journal of Biological Chemistry. 2013;288(11):7907-17.

38. Lehotzky A, Lau P, Tokési N, Muja N, Hudson LD, Ovádi J. Tubulin polymerization-promoting protein (TPPP/p25) is critical for oligodendrocyte differentiation. Glia. 2010;58(2):157-68.
39. Preusser M, Lehotzky A, Budka H, Ovádi J, Kovács GG. TPPP/p25 in brain tumours: expression in non-neoplastic oligodendrocytes but not in oligodendroglioma cells. Acta Neuropathologica. 2006;113(2):213-5.
40. Kang JU, Koo SH, Kwon KC, Park JW, Kim JM. Gain at chromosomal region 5p15.33, containing TERT, is the most frequent genetic event in early stages of non-small cell lung cancer. Cancer Genetics and Cytogenetics. 2008;182(1):1-11.
41. Inokawa Y, Sonohara F, Kanda M, Hayashi M, Nishikawa Y, Sugimoto H, et al. Correlation Between Poor Prognosis and Lower TPPP Gene Expression in Hepatocellular Carcinoma. Anticancer Research. 2016;36(9):4639-46.
42. Fjorback AW, Sundbye S, Dächsel JC, Sinning S, Wiborg O, Jensen PH. P25α/TPPP expression increases plasma membrane presentation of the dopamine transporter and enhances cellular sensitivity to dopamine toxicity. FEBS Journal. 2011;278(3):493-505.
43. Haakenson J, Zhang X. HDAC6 and Ovarian Cancer. International Journal of Molecular Sciences. 2013;14(5):9514-35.
44. Fukushima N, Furuta D, Hidaka Y, Moriyama R, Tsujiuchi T. Post-translational modifications of tubulin in the nervous system. Journal of Neurochemistry. 2009;109(3):683-93.
45. Hubbert C, Guardiola A, Shao R, Kawaguchi Y, Ito A, Nixon A, et al. HDAC6 is a microtubule-associated deacetylase. Nature. 2002;417(6887):455-8.
46. Tokesi N, Lehotzky A, Horvath I, Szabo B, Olah J, Lau P, et al. TPPP/p25 Promotes Tubulin Acetylation by Inhibiting Histone Deacetylase 6. Journal of Biological Chemistry. 2010;285(23):17896-906.
47. Iaconelli J, Huang JH, Berkovitch SS, Chattopadhyay S, Mazitschek R, Schreiber SL, et al. HDAC6 Inhibitors Modulate Lys49 Acetylation and Membrane Localization of β-Catenin in Human iPSC-Derived Neuronal Cells. ACS Chemical Biology. 2015;10(3):883-90.
48. Li Y, Zhang X, Polakiewicz RD, Yao TP, Comb MJ. HDAC6 Is Required for Epidermal Growth Factor-induced -Catenin Nuclear Localization. Journal of Biological Chemistry. 2008;283(19):12686-90.
49. Shan B, Yao Tp, Nguyen HT, Zhuo Y, Levy DR, Klingsberg RC, et al. Requirement of HDAC6 for Transforming Growth Factor- 1-induced Epithelial-Mesenchymal Transition. Journal of Biological Chemistry. 2008;283(30):21065-73.
50. Hsieh TH, Tsai CF, Hsu CY, Kuo PL, Lee JN, Chai CY, et al. Phthalates Stimulate the Epithelial to Mesenchymal TransitionThrough an HDAC6-Dependent Mechanism in Human BreastEpithelial Stem Cells. Toxicological Sciences. 2012;128(2):365-76.
51. Gelmon K. The taxoids: paclitaxel and docetaxel. The Lancet. 1990;344(8932):1267-72.

52. Pascucci L, Coccè V, Bonomi A, Ami D, Ceccarelli P, Ciusani E, et al. Paclitaxel is incorporated by mesenchymal stromal cells and released in exosomes that inhibit in vitro tumor growth: A new approach for drug delivery. Journal of Controlled Release. 2014;192:262-70.
53. Lopes NM, Adams EG, Pitts TW, Bhuyan BK. Cell kill kinetics and cell cycle effects of taxol on human and hamster ovarian cell lines. Cancer Chemother Pharmcol 1993;32:235-42.
54. Meng H, MeiyingWang, Liu H, Liu X, Situ A, Wu B, et al. Use of a Lipid-Coated Mesoporous Silica Nanoparticle Platform for Synergistic Gemcitabine and Paclitaxel Delivery to Human Pancreatic Cancer in Mice. ACSNANO. 2015;9(4):3540-57.
55. Bu H, He X, Zhang Z, Yin Q, Yu H, Li Y. A TPGS-incorporating nanoemulsion of paclitaxel circumvents drug resistance in breast cancer. International Journal of Pharmaceutics. 2014;471(1-2):206-13.
56. Kinoshita JUN, Fushida S, Tsukada T, Oyama K, Watanabe T, Shoji M, et al. Comparative study of the antitumor activity of Nab-paclitaxel and intraperitoneal solvent-based paclitaxel regarding peritoneal metastasis in gastric cancer. Oncology Reports. 2014;32(1):89-96.

Supplementary Material

Supplementary Figure 1. Schematic model illustrating the role of EBV-miR-BART12 in regulating NPC migration and invasion by targeting TPPP1.

Supplementary Figure 2.A The expression of TPPP1 was detected in 5-8F, AGS, and C666-1 cells after transfection or co-transfection of EBV-miR-BART12 mimics, EBV-miR-BART12 inhibitors, siTPPP1, or the TPPP1 overexpression vectors. B. The upper lane is representative images of

visible nodules on the surface of mouse lung. And arrows indicate clusters of tumor cells colonized from vein tail to lung. The lower lane is representative images of sections of lung tissues with HE staining.

Supplementary file 1. Primers used for qRT-PCR or constructions, inhibitors and siRNAs.PDF

The table including the sequences of the primers, inhibitors and siRNAs

Supplementary file 2. Prediction of target genes of EBV-miR-BART12 by the RepTar software.PDF

The table of prediction of target genes of EBV-miR-BART12 by the RepTar software.

Supplementary file 3. Negative genes in nasopharyngeal carcinoma of GSE12452.PDF

The table of negative expressed gene list in NPC compared to the non-tumor tissue in GSE12452 analyzed by SEM

Figures

Figure 1

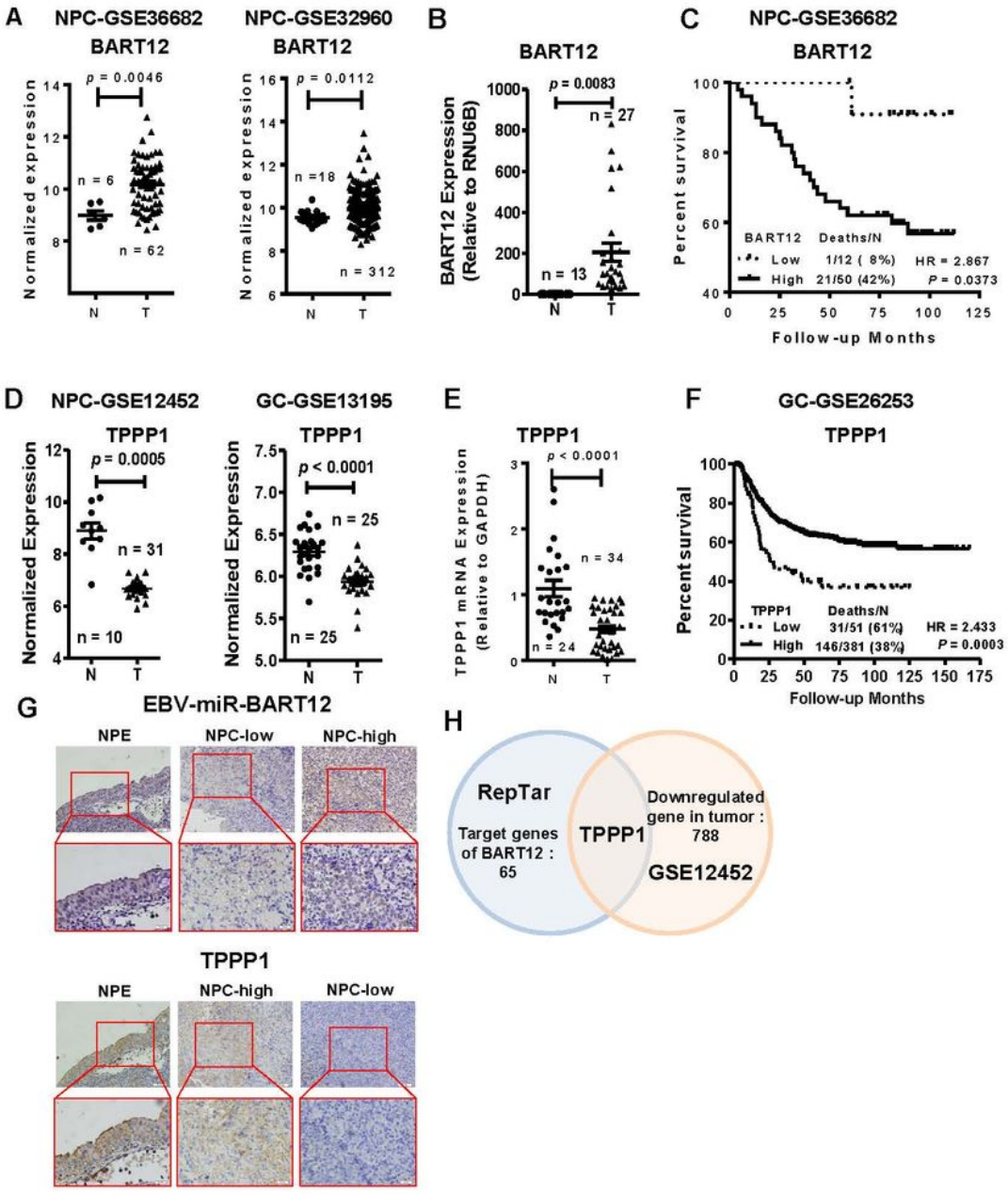

Figure 1

The expression and the correlation of EBV-miR-BART12 and TPPP1 gene in NPC. NPE, nasopharyngeal epithelial tissue; NPC, nasopharyngeal carcinoma; N, Normal gastric mucosa; GC, gastric cancer A. The expression of EBV-miR-BART12 in NPC tissues was analyzed in NPC GEO data sets GSE36682 (NPE = 6, NPC = 62) and GSE32960 (NPE = 18, NPC = 312). B. The qRT-PCR experiments were performed to detect the expression of BART12 in NPC biopsies (NPE = 13, NPC = 27). C. Overall survival analysis of NPC

patients with low and high EBV-miR-BART12 expression using a Kaplan-Meier curve in the NPC GEO dataset GSE36682. D. The expression of TPPP1 in NPC tissues was analyzed in NPC GEO data sets GSE12452 (NPE = 10, NPC = 31) and the gastric cancer GEO dataset GSE13195 (N = 25, GC = 25). E. TPPP1 expression was validated in NPC biopsies (NPE = 24, NPC = 34) by qRT-PCR. F. Relapse-free survival analysis of NPC patients with low and high TPPP1 expression using a Kaplan-Meier curve in the gastric cancer GEO dataset GSE26253. G. The expression of EBV-miR-BART12 and TPPP1 were detected in NPC biopsies by in situ hybridization (ISH) and immunochemistry (IHC), respectively. H. Target mRNAs of EBV-miR-BART12 which were predicted by the bioinformatics software RepTar were overlapped with the genes which were found down-regulated in NPC in the GSE12452 chip data, the result is TPPP1 only.

Figure 2

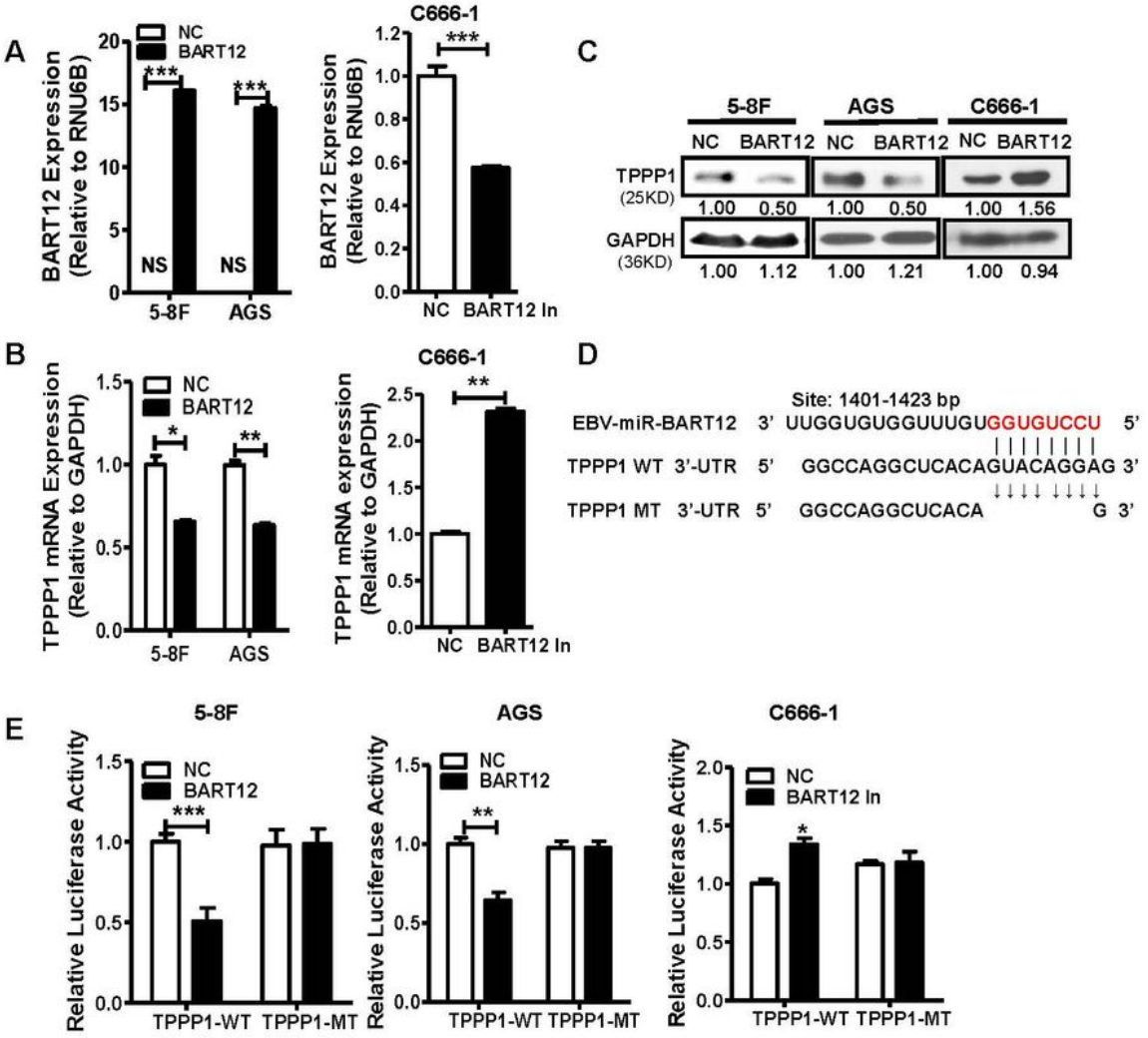

Figure 2

EBV-miR-BART12 inhibits TPPP1's expression through targeting its 3'-UTR. A. EBV negative cells 5-8F and AGS were transfected with EBV-miR-BART12 mimics (50 nM), and EBV positive cells C666-1 were performed with EBV-miR-BART12 inhibitors (50 nM) transfection for 36 h. The expression of EBV-miR-BART12 was detected by real-time PCR. B. The expression of TPPP1 at the RNA level was inhibited by EBV-miR-BART12 mimics after transfection in 5-8F and AGS. EBV-miR-BART12 inhibitors reduced its

expression in C666-1 cells with EBV-miR-BART12 inhibitors transfection. C. The expression of TPPP1 was detected in EBV negative 5-8F and AGS cells transfected with EBV-miR-BART12 mimics and EBV positive C666-1 cells with EBV-miR-BART12 inhibitors (50 nM) by western blotting. D. The binding site of EBV-miR-BART12 located on 1401-1423 bp of the TPPP1 3’-UTR was predicted by the bioinformatics software and constructed as the wild type luciferase reporter vector of TPPP1. The seed sequence of EBV-miR-BART12 was deleted to construct the mutant reported luciferase reporter vector of TPPP1. E. The luciferase was detected after EBV-miR-BART12 mimics or inhibitors, the luciferase reporter vector containing the wild type (TPPP1-WT) or mutant (TPPP1-MT), and the pRL-TK luciferase vector were co-transfected into 5-8F and AGS cells or C666-1 cells (*, $p < 0.05$; **, $p < 0.01$; ***, $p < 0.001$).

Figure 3

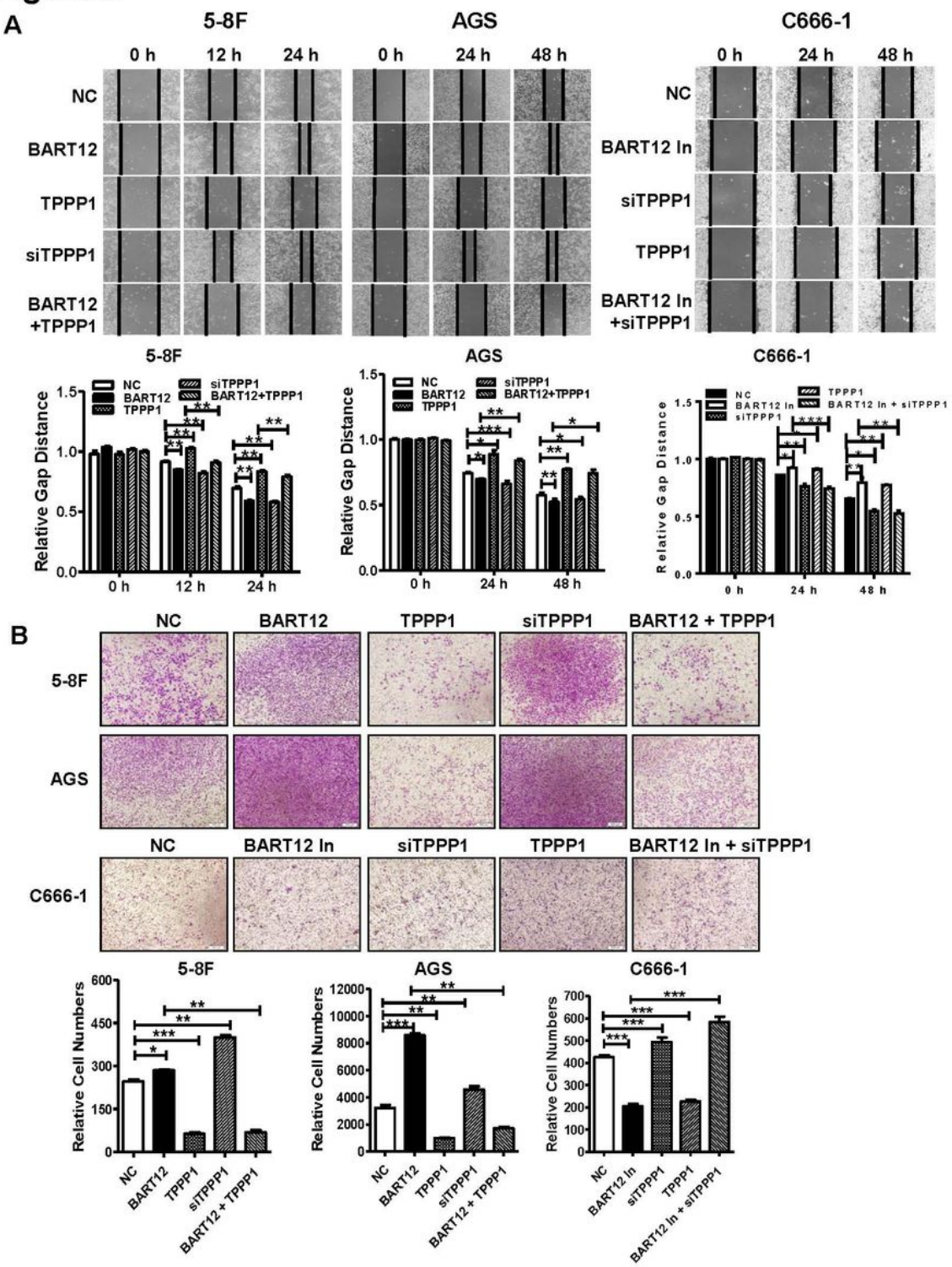

Figure 3

EBV-miR-BART12 promotes the migration and invasion of cancer cells by inhibiting the expression of TPPP1. The invasion (A) and migration (B) ability were measured after EBV-miR-BART12 mimics (BART12), the TPPP1 vector (TPPP1), TPPP1-siRNA (siTPPP1), or EBV-miR-BART12 mimics and the TPPP1 vector (BART12+TPPP1) transfection or co-transfection in 5-8F and AGS cells using the wound

healing method, and transwell respectively. And they were also measured in C666-1 cells after EBV-miR-BART12 inhibitors (BART12 In) were transfected (*, $p < 0.05$; **, $p < 0.01$; ***, $p < 0.001$.).

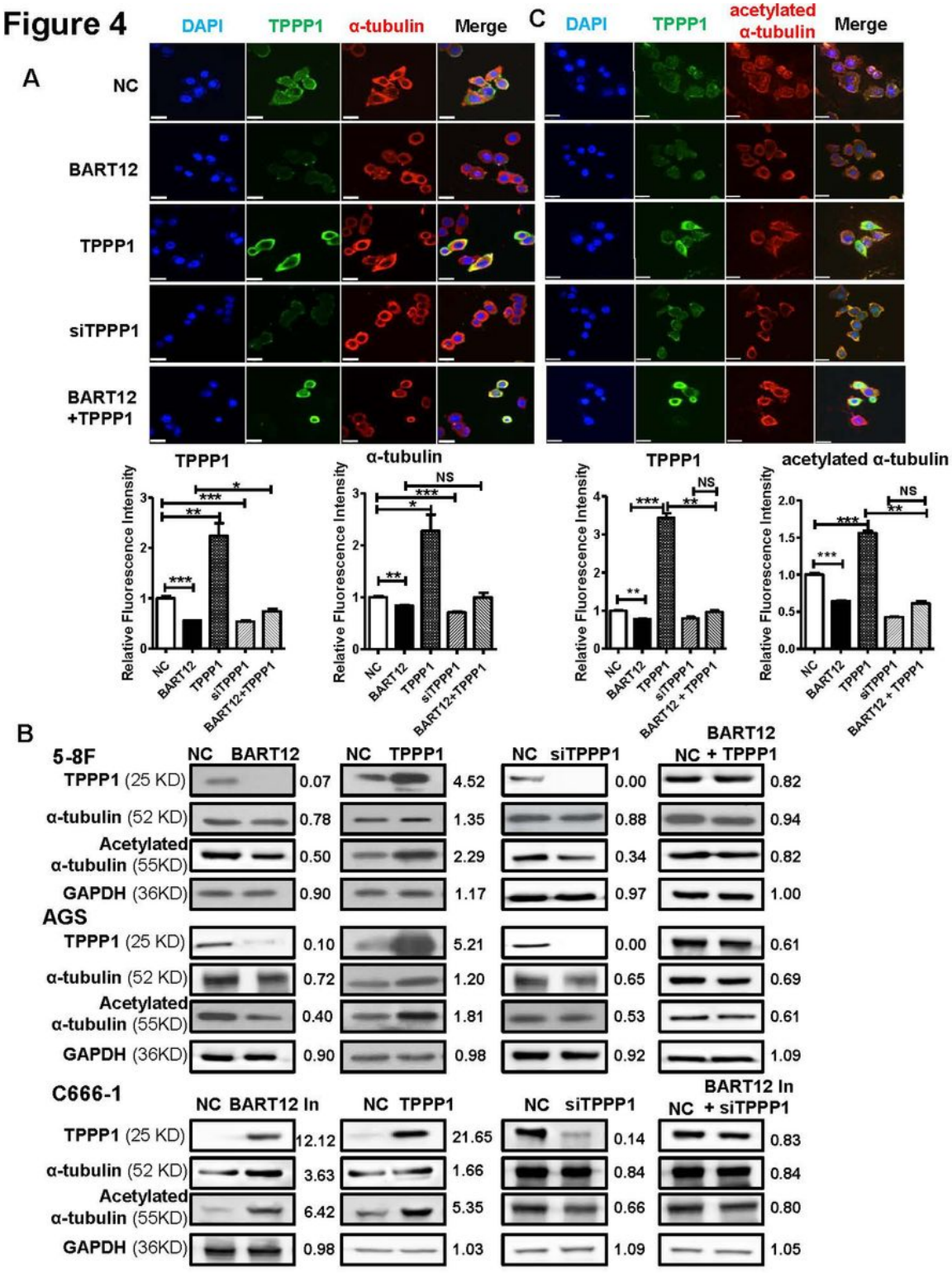

Figure 4

EBV-miR-BART12 decreases α-tubulin acetylation and affects the microtubules networks through down-regulating TPPP1 expression. A. The expression and distribution of α-tubulin was detected by immunofluorescence in 5-8F cells after EBV-miR-BART12 mimics (BART12), the TPPP1 vector (TPPP1),

TPPP1-siRNA (siTPPP1), or EBV-miR-BART12 mimics and the TPPP1 vector (BART12 + TPPP1) transfection or co-transfection, respectively. B. The expression of α-tubulin and acetylated-α-tubulin was detected by western blotting after EBV-miR-BART12 mimics (BART12), the TPPP1 vector (TPPP1), TPPP1-siRNA (siTPPP1), or EBV-miR-BART12 mimics and the TPPP1 vector (BART12 + TPPP1) transfection or co-transfection, respectively in 5-8F, AGS, or EBV-miR-BART12 inhibitor (BART12 In), the TPPP1 vector (TPPP1), TPPP1-siRNA (siTPPP1), or EBV-miR-BART12 inhibitors and siTPPP1 (BART12 In + siTPPP1) transfection in C666-1 cells. C. Immunofluorescence assay was performed to detect the expression and distribution of acetylated α-tubulin in 5-8F after EBV-miR-BART12 mimics (BART12), the TPPP1 vector (TPPP1), TPPP1-siRNA (siTPPP1), or EBV-miR-BART12 mimics and the TPPP1 vector (BART12 + TPPP1) transfection or co-transfection, respectively (*, $p < 0.05$; **, $p < 0.01$; ***, $p < 0.001$.).

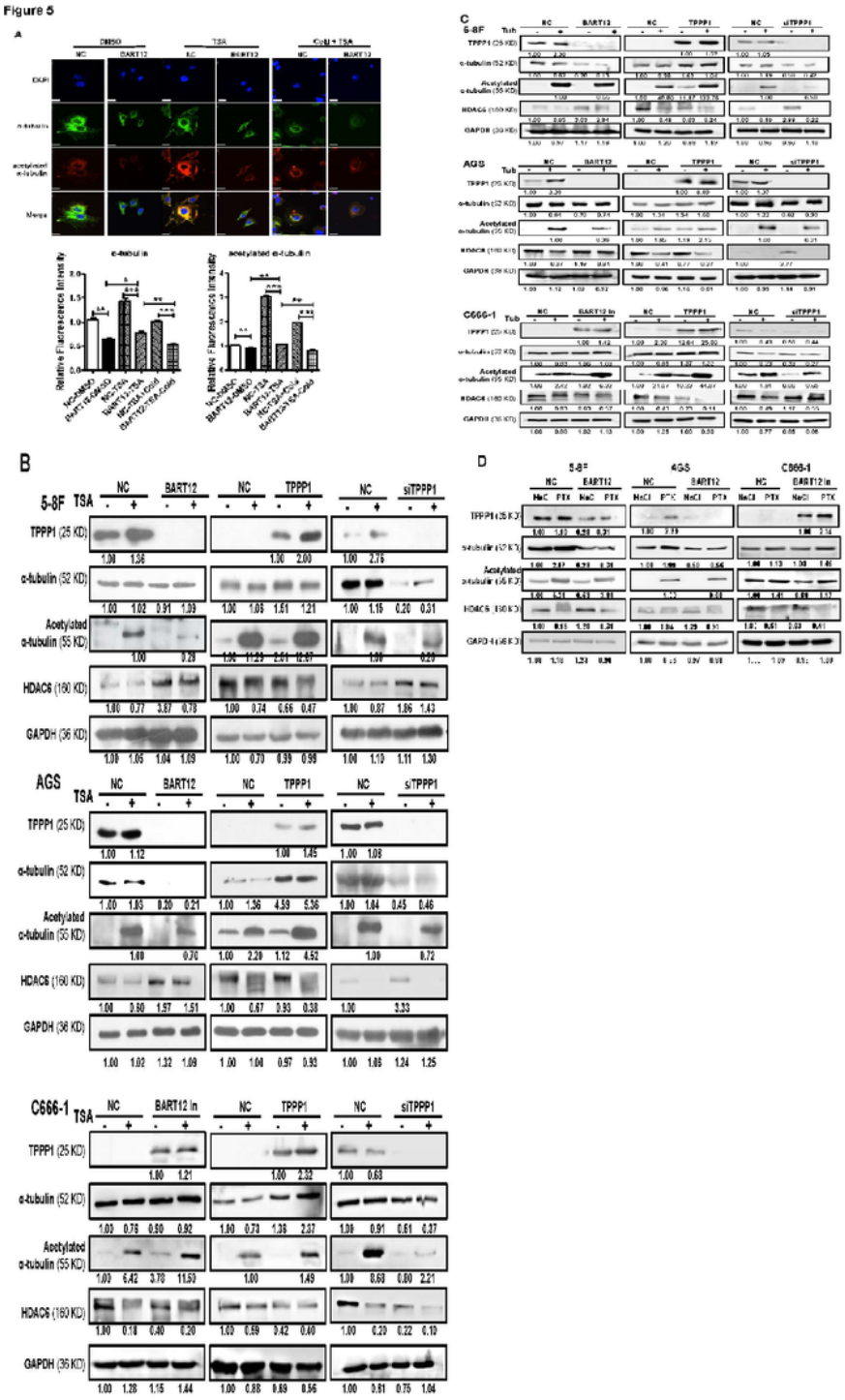

Figure 5

EBV-miR-BART12 reduces the influences of TSA on the expression of α-tubulin and acetylated-α-tubulin. A. 5-8F cells was treated with 240 nM TSA with or without cold for 24 h after EBV-miR-BART12 mimics (BART12) transfection. Immunofluorescence assay was used to detect the expression and distribution of the total α-tubulin and acetylated α-tubulin. B, C, and D. The expression of α-tubulin and acetylated α-tubulin were detected after TSA (B), Tub (C) or PTX (D) were added to treated with 5-8F and AGS cells

transfected EBV-miR-BART12 mimics (BART12) or C666-1 cells transfected EBV-miR-BART12 inhibitor (BART12 In). (*, p < 0.05; **, p < 0.01; ***, p < 0.001.).

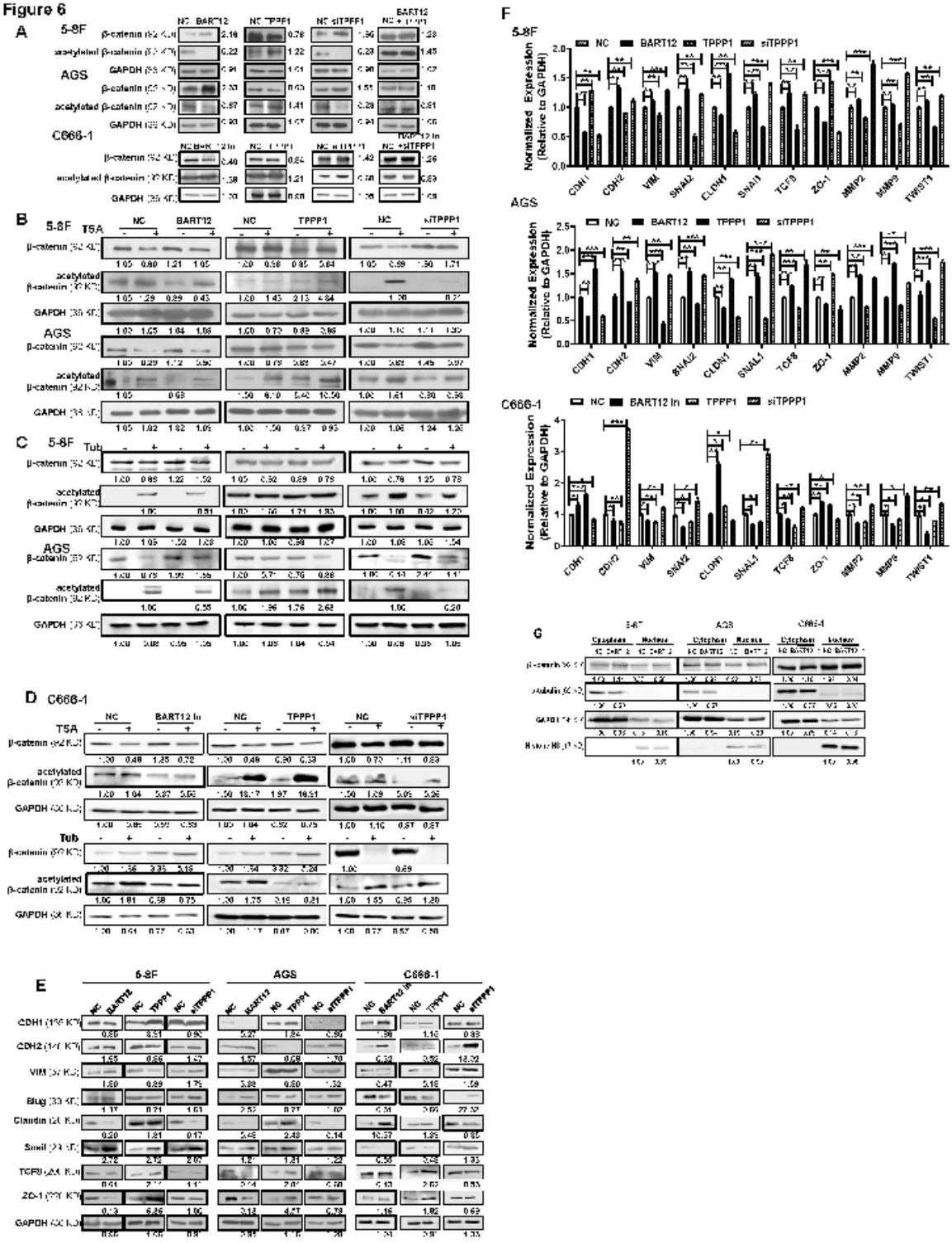

Figure 6

EBV-miR-BART12 induces the EMT process by restraining the inhibitory effect of TPPP1 on β-catenin. A. Western blotting was performed to examine the expression of the total and acetylation of β-catenin in 5-8F and AGS cells after transfected with EBV-miR-BART12 mimics (BART12), the TPPP1 overexpression

(TPPP1), siTPPP1, or transfected EBV-miR-BART12 mimics and the TPPP1 overexpression vector, and C666-1 with EBV-miR-BART12 inhibitors (BART12 In), the TPPP1 overexpression TPPP1), siTPPP1, or EBV-miR-BART12 inhibitors and siTPPP1. B and C. The expression of the total and acetylation of β-catenin were detected by western blotting in 5-8F and AGS cells transfected with EBV-miR-BART12 mimics (BART12), the TPPP1 overexpression (TPPP1), or siTPPP1 before TSA (B) or Tub (C) were treated for 24h. Western blotting showed that EBV-miR-BART12 reduced the acetylation of β-catenin treated with 240 nM TSA for 24 hours through inhibiting TPPP1 in 5-8F and AGS. D. The expression of the total and acetylation of β-catenin were detected by western blotting in C666-1 cells transfected with EBV-miR-BART12 inhibitor (BART12 In), the TPPP1 overexpression (TPPP1), or siTPPP1 before TSA or Tub were treated for 24 h. E and F. The expression levels of epithelial markers and mesenchymal markers were examined by western blot analysis (E) and real-time PCR (F). G. The expression of β-catenin in the cytoplasm and in the nucleus was elevated by western blotting. GAPDH was used as an internal control. Histone H3 was used as a nucleus control (*, $p < 0.05$; **, $p < 0.01$; ***, $p < 0.001$.).

Supplementary Files

This is a list of supplementary files associated with this preprint. Click to download.

- Subpplementarytable3.pdf
- BART12TPPP1figures.pdf
- Subpplementarytable2.pdf
- Subpplementarytable1.pdf
- SupplementaryFigures.pdf